OPTIMAL LIFTING ASCENT TRAJECTORIES FOR THE SPACE SHUTTLE

By Timothy R. Rau and Jarrell R. Elliott
NASA Langley Research Center
Hampton, Virginia

INTRODUCTION

For many years trajectory analysts have been promoting the idea of using optimal lifting or optimal pointing trajectories as a way of improving the performance capabilities of boost-launch systems. However, prior to the space shuttle, the launch systems being built were not well suited to the use of such trajectories; the systems were incapable of producing substantial lift and were structurally incapable of withstanding the additional airloads brought about by optimal pointing of the thrust vector. Fortunately the space shuttle has these necessary capabilities and thus it provides the trajectory analyst with a new opportunity to demonstrate that the use of optimal lifting and pointing trajectories, as compared to ballistic trajectories, can materially increase the performance capabilities of boost-launch systems. Previous studies, such as reference 1, have parametrically studied the effect of adding wing areas to a boost-launch vehicle. This paper summarizes the performance gains which are possible through the use of optimal trajectories for a particular shuttle configuration and points out how these gains are produced.

CONFIGURATION STUDIED

A three-view drawing of the shuttle configuration studied is shown in figure 1. This is a fully reusable configuration in which the orbiter stage is mounted piggy-back style on the booster stage, both having delta wings. The distance from the nose of the orbiter to the tail of the booster is about 90 meters. The wing area of the orbiter is about 620 square meters while that of the booster is about 790 square meters. For comparison, the wing area of the Boeing 747 is about 520 square meters. Figure 2 shows a superposed planview of the shuttle over that of the Boeing 747.

Three basic missions are considered in the sizing of the shuttle: a polar orbit mission, a 55° orbit inclination mission, and a 28.5° orbit inclination mission. A polar orbit mission requirement of 18 140 kilograms (40 000 pounds) payload to a 50- by 100-nautical mile orbit sized the orbiter and booster elements. The weights of these two elements are as shown on figure 1 with the gross launch weight being around 2.29 million kilograms or about 5 million pounds.

SHUTTLE CONFIGURATION STUDIED

GROSS LIFT-OFF WEIGHT 2.29 MILLION kg
BOOSTER LIFT-OFF WEIGHT 1.90 MILLION kg
ORBITER LIFT-OFF WEIGHT 0.39 MILLION kg

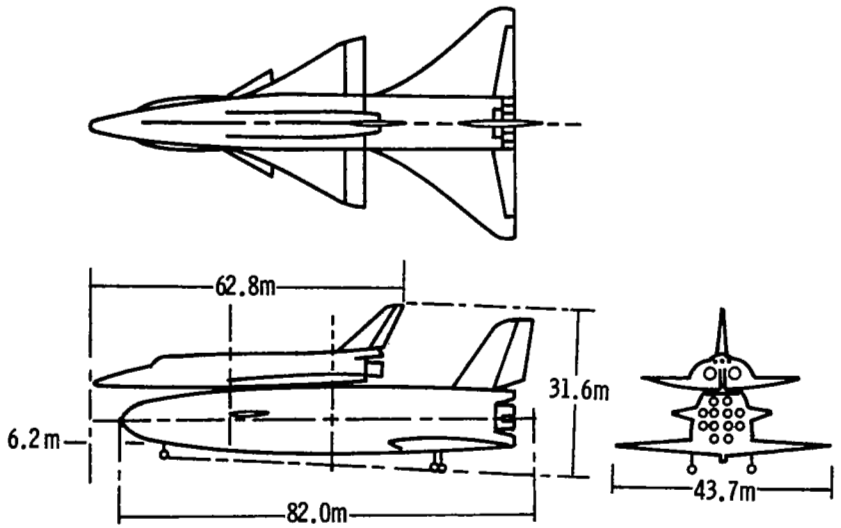

Figure 1

SHUTTLE-BOEING 747 COMPARISON

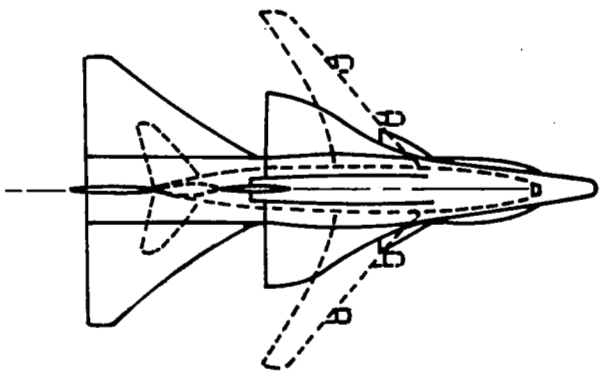

Figure 2

SHUTTLE CHARACTERISTICS

The thrust to weight ratios of the booster and orbiter at ignition are 1.3 and 1.5, respectively. In modeling this configuration for the trajectory computation program one of the ground rules followed was that the axial acceleration of the launch vehicle would not be allowed to exceed 3g. This required engine throttling in each of the stages. Typical thrust and weight time histories are shown in figure 3. Additional features of the shuttle configuration are presented in figure 4. Another ground rule followed was that the thrust axis be directed through the vehicle center of gravity.

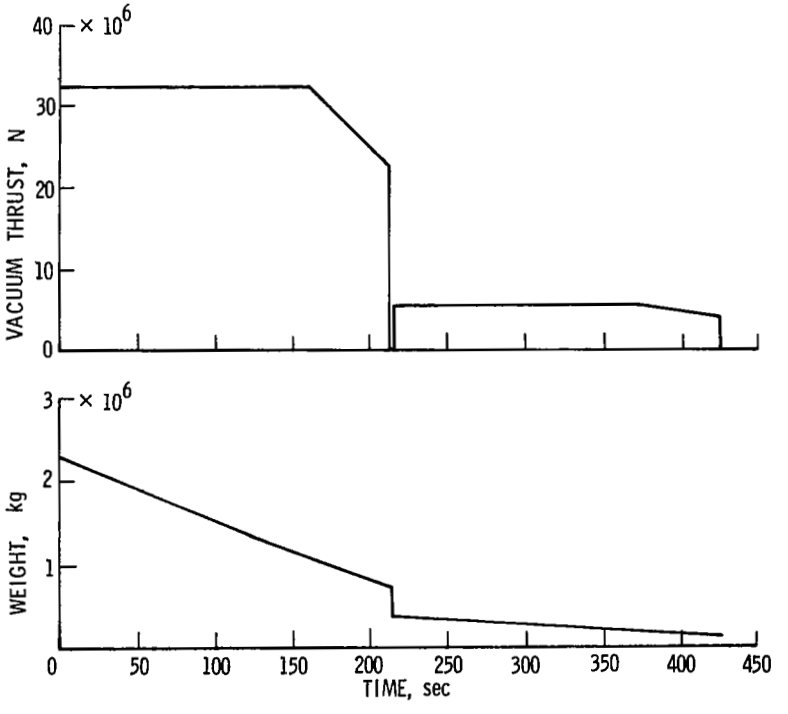

Figure 3

SHUTTLE CHARACTERISTICS

Characteristic	Stage	
	Booster	Orbiter
Number of engines	12	2
Specific impulse (vacuum), sec	439	459
Nozzle exit area, m^2	28.2	20.2
Aerodynamic reference area, m^2	785	618
Propellant weight, kg	1253×10^3	252×10^3
Landing weight, kg	290×10^3	122×10^3

Figure 4

LAUNCH CALCULATIONS

As described in figure 5, a point mass trajectory optimization program, based on the steepest ascent technique of iterative trajectory optimization, was used for calculating the trajectories. The program, described in reference 2, provided a fairly exact mathematical model of the shuttle. This program is quite versatile and is capable of optimizing and simultaneously satisfying a wide variety of constraints. Examples are to constrain certain portions of the flight to fly a specified angle-of-attack program or to constrain an airload parameter, the product of dynamic pressure and the angle of attack ($\bar{q}\alpha$), to be below a specified limiting value. The program was operated with various constraints for this study but was always operated to maximize the payload for a prescribed propellant loading. Vehicle launches were assumed to take place from Kennedy Space Center. The earth model used was a spherical rotating earth with the 1959 ARDC model atmosphere (reference 3).

LAUNCH CALCULATIONS

1. USED ITERATIVE STEEPEST ASCENT METHOD
2. CALCULATED THE MAXIMUM PAYLOAD FOR FIXED STRUCTURE AND FUEL LOADING
3. LIMITED THE AXIAL ACCELERATION TO 3g OR LESS
4. DIRECTED THE THRUST VECTOR THROUGH THE VEHICLE C. G.
5. IMPOSED $(\bar{q}\alpha)_{max}$ LIMITS ON LIFTING TRAJECTORIES

Figure 5

AERODYNAMIC DATA

Typical aerodynamic data in the form of lift coefficient plotted against drag coefficient for several Mach numbers are shown in figure 6. One of the characteristics of this configuration is that it has a positive aerodynamic lift coefficient at zero angle of attack so that it was necessary to program the angle of attack to obtain a ballistic, or nonlifting, trajectory during atmospheric flight for comparison with the lifting trajectories. This characteristic also casts some doubt upon the validity of using the airload parameter $(\bar{q}\alpha)_{max}$ as a basic parameter in structural considerations since appreciable lift is generated on a zero angle-of-attack trajectory. This will become more apparent in the results to follow.

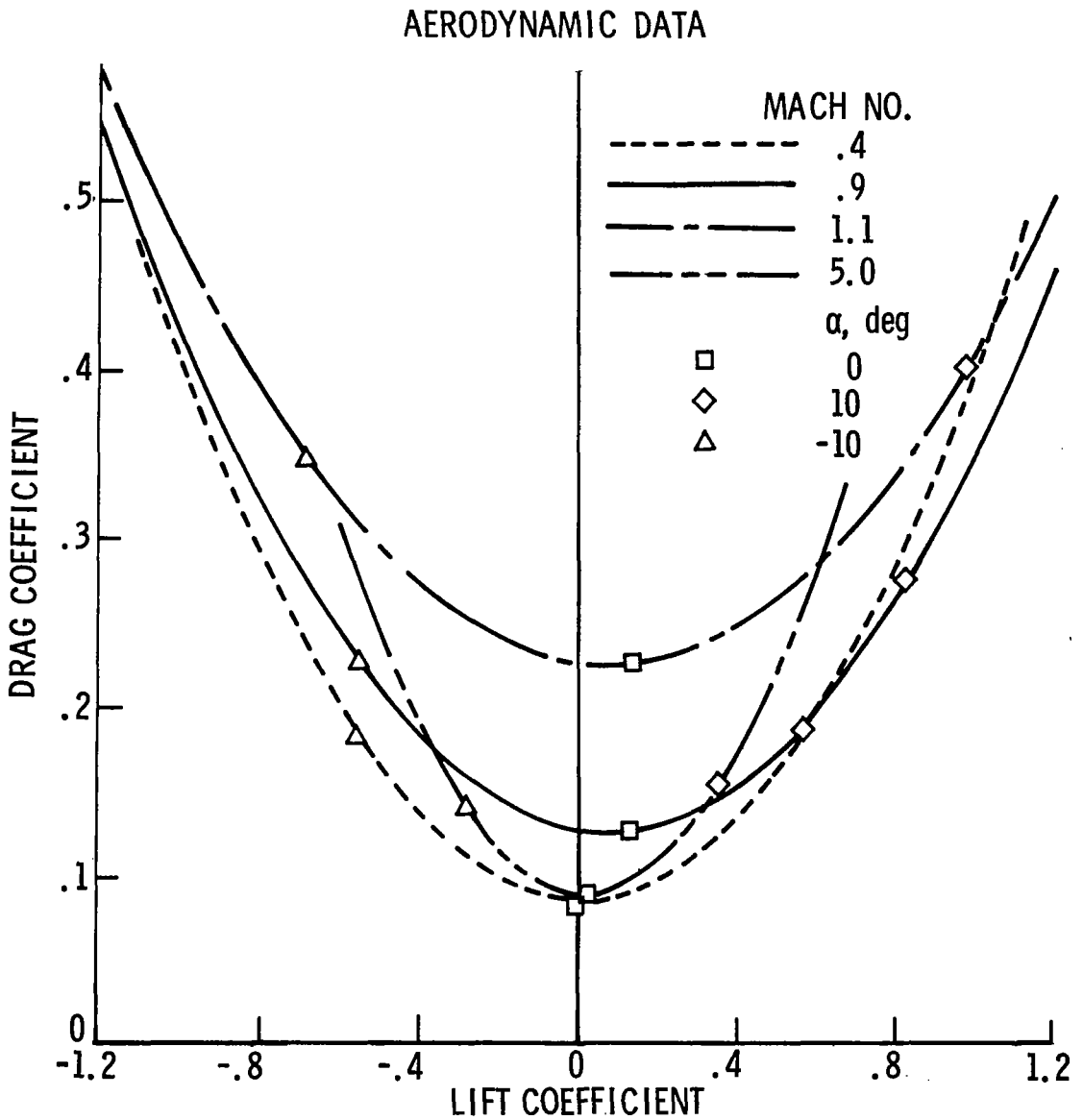
AERODYNAMIC DATA
MACH NO.
.4
.9
1.1
5.0
α, deg
0
10
-10
DRAG COEFFICIENT
.5
.4
.3
.2
.1
0
-1.2
-.8
-.4
0
.4
.8
1.2
LIFT COEFFICIENT

Figure 6

SHUTTLE MISSION PAYLOAD

Payload improvements possible through the use of optimal lifting trajectories for the three different missions are shown in figure 7. The payload to a 50- by 100-nautical-mile orbit is plotted against mission in terms of the mission orbit inclination. Three curves are shown: the lower one for a nonlifting trajectory, the upper one for an unconstrained lifting trajectory, and the third for a lifting trajectory constrained to a maximum allowable $q\alpha$.

Note that the polar mission, nonlifting data point indicates that 18 140 kilograms (40 000 pounds) payload can be orbited. The payload is roughly doubled by launching due east from Kennedy Space Center indicated at the 28.5° orbit inclination point.

For the unconstrained optimal-lifting polar trajectory, approximately 22 640 kilograms (50 000 pounds) payload can be orbited. This represents about 4500 kilograms (10 000 pounds) or a 25 percent increase in payload capability for this mission. For other missions, the payload improvement increases with decreasing orbit inclination to a maximum of 6000 kilograms (13 200 pounds) at 28.5° inclination.

The performance gain indicated by the unconstrained curve is probably impossible to achieve since it requires the vehicle to pitch down at very high pitch rates immediately after launch (a pitch attitude of about 50° at 15 seconds into flight is required). Also, the vehicle would have to be designed to withstand $q\alpha$ airloads in excess of 345 000 deg-N/m^2 (about 7200 deg-psf), where current design values are 134 000 deg-N/m^2 (2800 deg-psf), and the wing body must be structured to carry up to 2.1 million kilograms (4.6 million pounds) of lift. This is probably too much to expect. However, it is possible to achieve a large part of the performance improvement by simply constraining the $(\overline{q\alpha})_{max}$ to be below a specified value. The curve labeled "constrained" limited $(\overline{q\alpha})_{max}$ to 134 000 deg-N/m^2 and, as can be seen for the polar design point mission, increased payload by about 3500 kilograms (7700 pounds) as compared to 4500 kilograms for the unconstrained trajectory. Similar results are shown for the other missions.

A part of these payload improvements may be attributable to the ability of the vehicle to efficiently use its lifting capability and a part to the ability to point the thrust vector in the optimum direction. Later in the paper the portion of the improvement due to lifting and the portion due to thrust pointing will be separately evaluated.

SHUTTLE MISSION PAYLOAD CAPABILITY

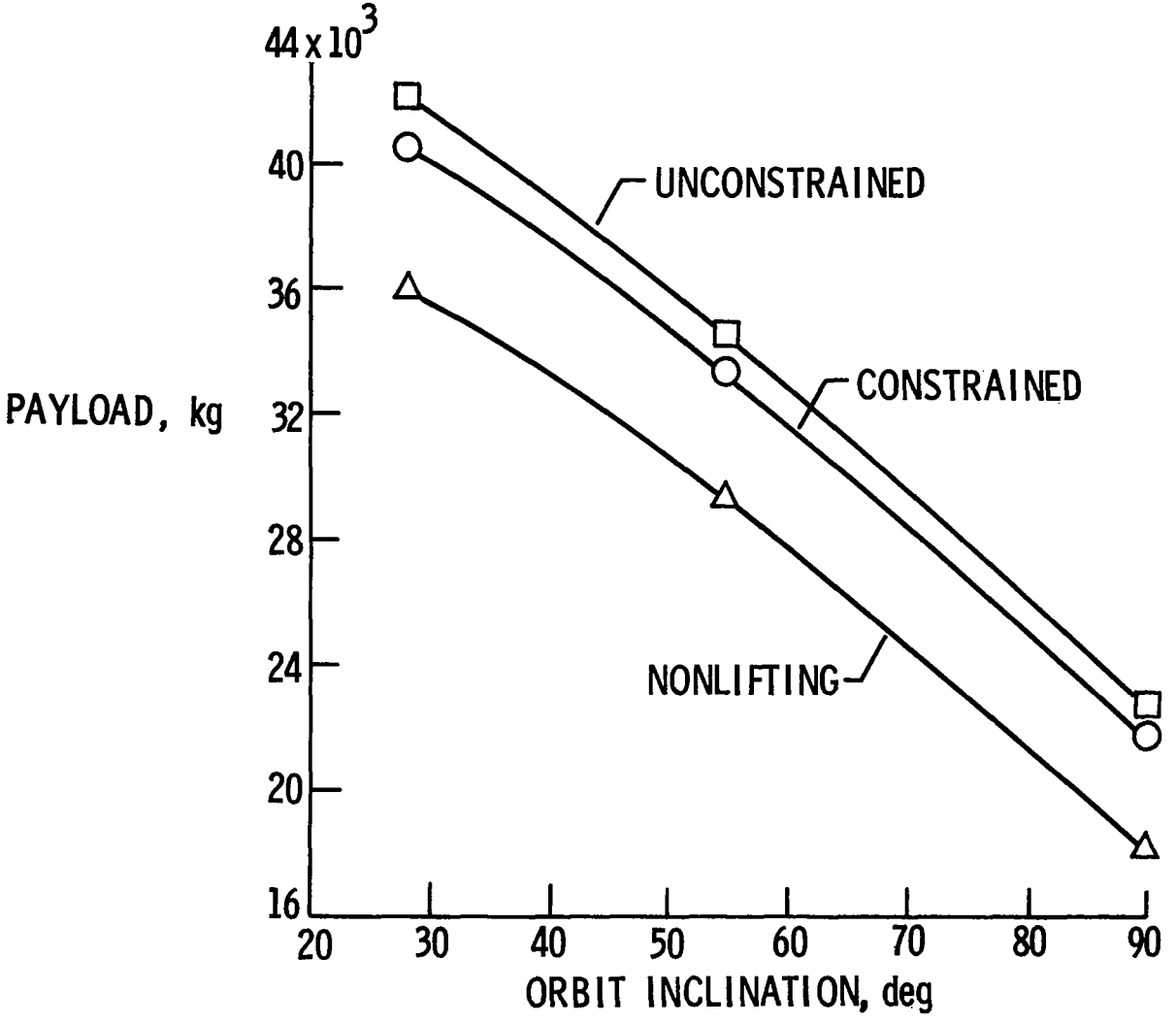

Figure 7

PAYLOAD FOR POLAR ORBIT

For the moment, however, the polar orbit mission will be examined in more detail. In particular, since $\bar{q}\alpha$ is used as a basic design parameter, the way that payload varies as maximum allowable $q\alpha$ is increased will be shown. In figure 8 the payload to orbit for the polar mission is plotted against $(\bar{q}\alpha)_{max}$. Also shown on the plot is the payload injected using a nonlifting trajectory. As can be seen, the payload obtainable with $(\bar{q}\alpha)_{max} = 0$ shows a substantial payload increase over that of the nonlifting trajectory. This is because of the lift generated at zero angle of attack, as previously mentioned. An interesting characteristic of this curve is the bend in the vicinity of $(\bar{q}\alpha)_{max} = 55\ 000$ deg-N/m^2. This indicates that perhaps a good design value of $(\bar{q}\alpha)_{max}$ for lifting trajectories, for this configuration, might be around 55 000 to 65 000 deg-N/m^2 (1200 to 1400 deg-psf) which is about half of the current design guideline. Of course, this number would have to be increased to provide for off-nominal trajectories, winds, and so forth. However, the horizontal wind shear problem is not as severe as one might think because the flight-path angles of the lifting trajectories are considerably lower in the region of maximum $\bar{q}\alpha$ than those of the ballistic trajectory. As a consequence, the lifting trajectories are less sensitive to horizontal wind shear.

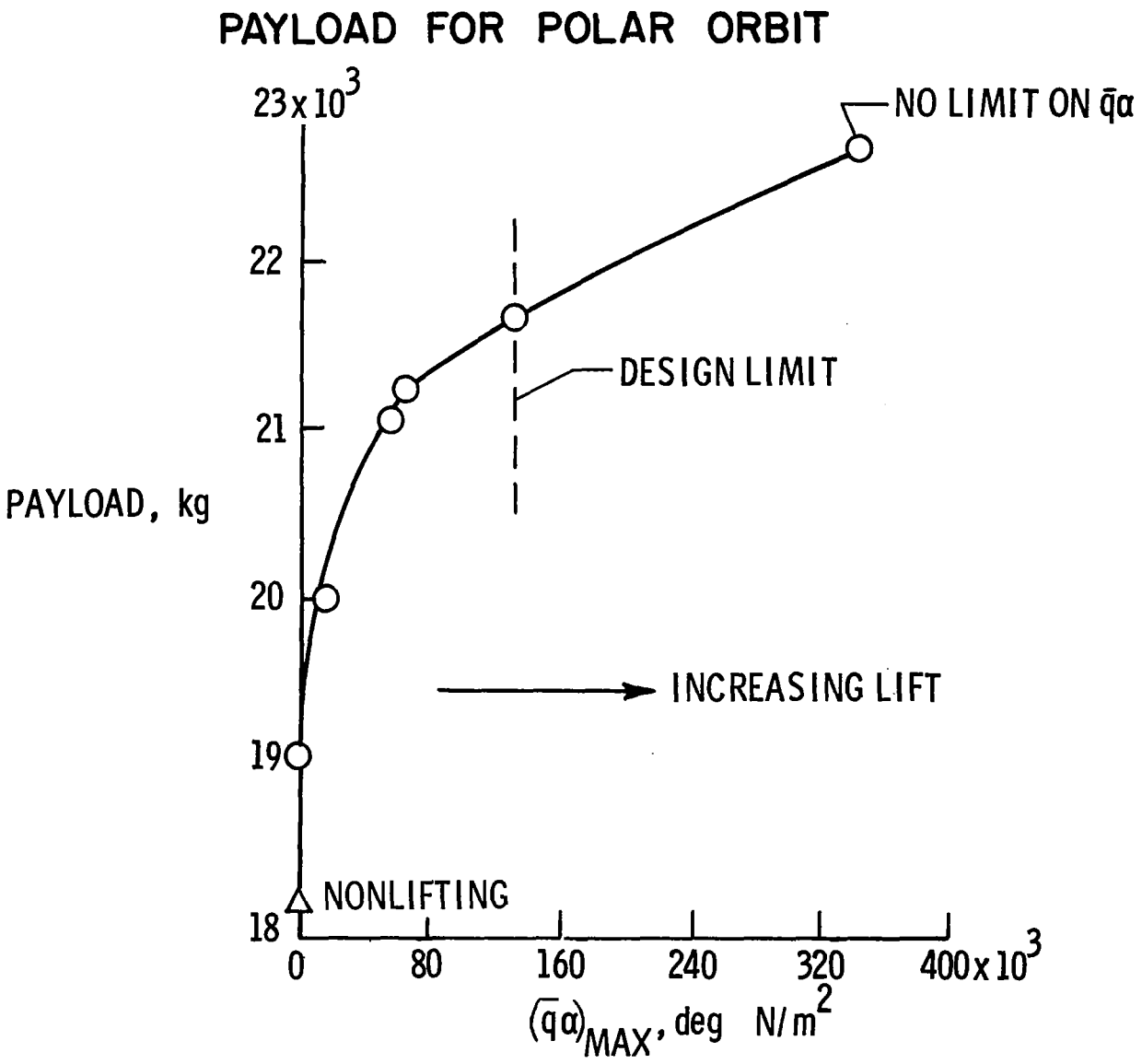
PAYLOAD FOR POLAR ORBIT
23x10^3
22
21
20
19
18
PAYLOAD, kg
NO LIMIT ON q̄α
DESIGN LIMIT
INCREASING LIFT
NONLIFTING
0
80
160
240
320
400x10^3
(q̄α)MAX, deg N/m^2

Figure 8

VELOCITY LOSSES

A part of the possible payload improvement shown is due to optimal pointing of the thrust vector and a part is due to optimal use of the lift capability of the configuration. Both of these factors are important in the reduction of the major source of velocity loss, that loss due to gravity. The major loss sources which prevent the realization of the ideal ΔV of a configuration are: gravity loss, drag loss, engine back pressure loss, and thrust vectoring loss. In order to show how these losses vary as the lift force changes, a new parameter is required. This new parameter is shown on the abscissa of figure 9 and is simply the integrated lift acceleration. The ordinate is the ΔV loss and the data points correspond to the non-lifting trajectory and a $(\bar{q}\alpha)_{max}$ of 0, 19 000, 67 000, 134 000, and 345 000 deg-N/m^2 moving from left to right. Both the back pressure loss and the thrust vectoring loss are relatively small, between 60 and 90 m/s, and are relatively insensitive to trajectory shaping so that not too much can be done about them. The gravity loss ΔV, however, is about 1290 m/s (about one-seventh of the ideal ΔV) for a ballistic trajectory and the drag loss is about 135 m/s. An optimal trajectory will tend to make the best use of thrust pointing and lift generation in order to reduce the total velocity loss. This is accomplished by reducing the gravity loss but is accompanied by increases in the drag loss. As shown on the total curve, the gravity loss decreases are just about equal to the increases in drag, back pressure, and thrust vectoring losses for large $(\bar{q}\alpha)_{max}$ values, indicating that no further payload increases are possible.

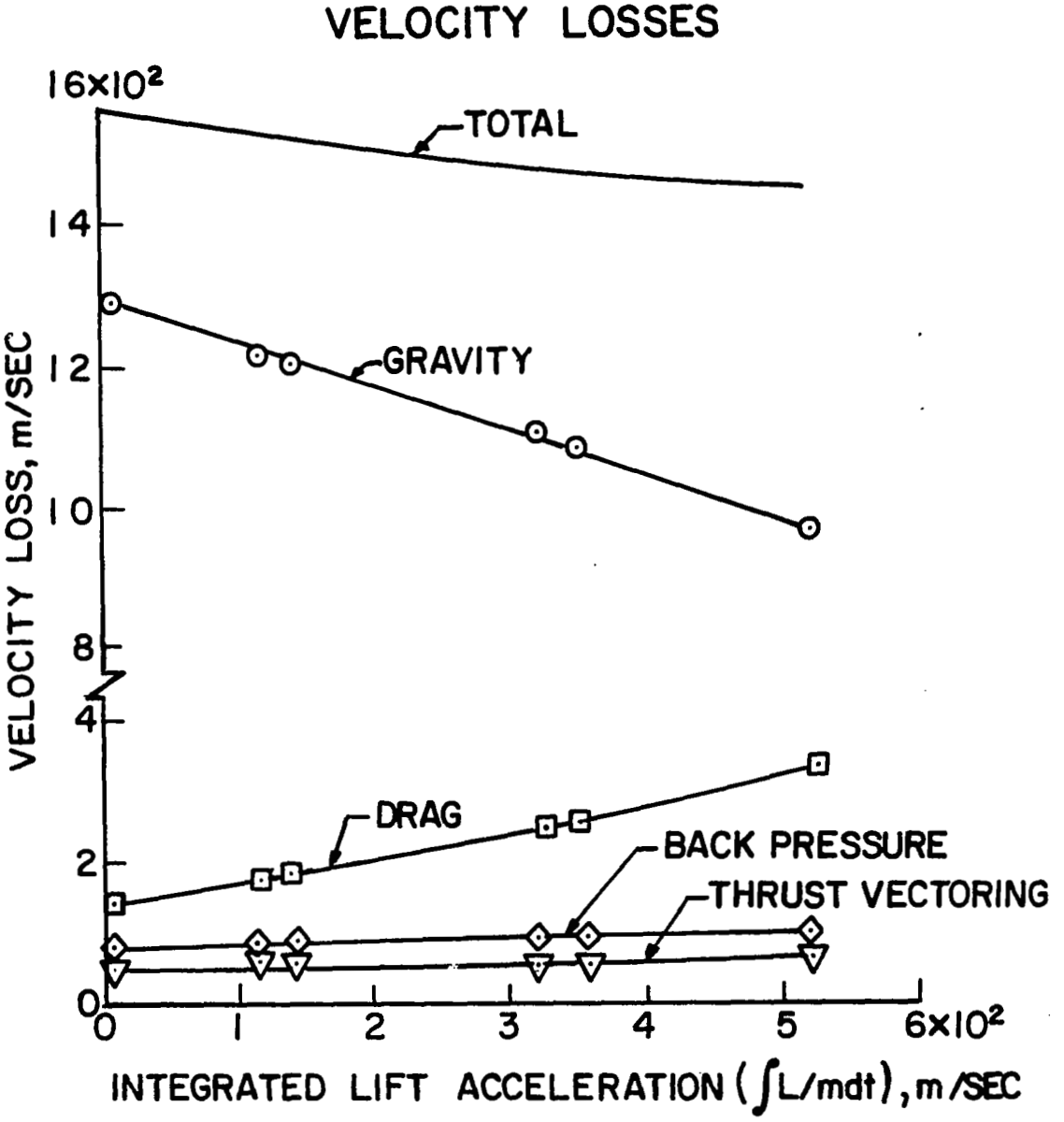
VELOCITY LOSSES
16×10²
14
12
10
8
4
2
0
VELOCITY LOSS, m/SEC
TOTAL
GRAVITY
DRAG
BACK PRESSURE
THRUST VECTORING
0
1
2
3
4
5
6×10²
INTEGRATED LIFT ACCELERATION (∫L/mdt), m/SEC

Figure 9

VELOCITY LOSS SOURCES

In order to further illustrate this mechanism, figure 10 shows time-history comparisons during booster burn between gravity loss acceleration ($g \sin \gamma$) and drag acceleration (D/m) for three trajectories: the nonlifting or ballistic, the constrained lifting, and the unconstrained lifting optimals. As can be seen in the time histories, since the gravity term is proportional to $\sin \gamma$, the tendency of the optimal lifting trajectories is to decrease the flight-path angle very quickly and thereby reduce the gravity acceleration as soon as possible. This is accomplished at some expense in the drag term.

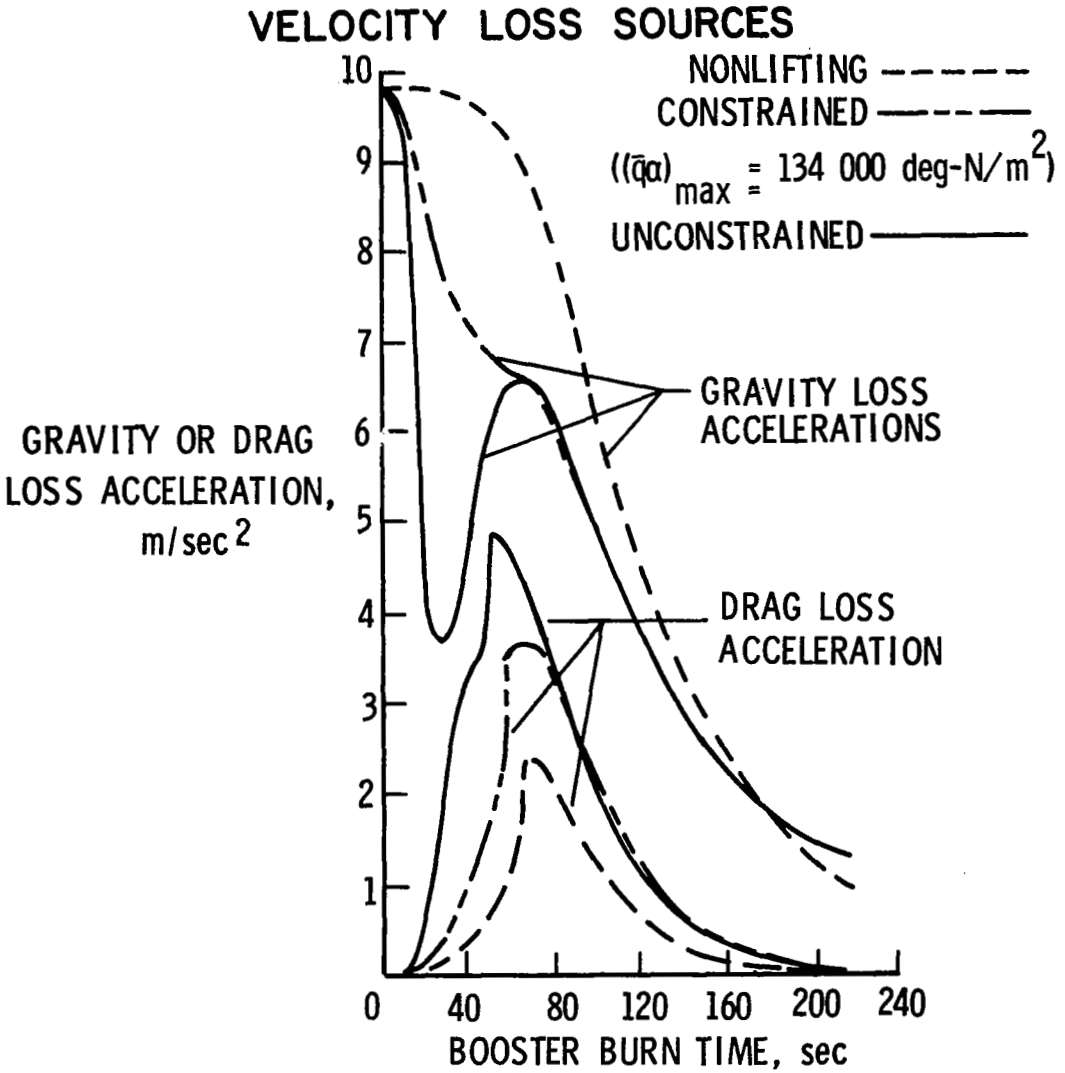
VELOCITY LOSS SOURCES
NONLIFTING
CONSTRAINED
$((\bar{q}\alpha)_{max} = 134\ 000$ deg-N/m^2)
UNCONSTRAINED
GRAVITY LOSS ACCELERATIONS
DRAG LOSS ACCELERATION
GRAVITY OR DRAG LOSS ACCELERATION, m/sec^2
10
9
8
7
6
5
4
3
2
1
0
40
80
120
160
200
240
BOOSTER BURN TIME, sec

Figure 10

LAUNCH TRAJECTORIES

In figure 11, flight-path angle, velocity, and altitude during booster burn are shown for each of the trajectories. As expected, the optimal lifting trajectories fly lower and faster than the nonlifting. Note also the much lower flight-path angles of the lifting trajectories which makes them less sensitive to horizontal wind shear during the period of $(\bar{q}\alpha)_{max}$, generally occurring around 40 seconds. In figure 12, time histories for lift, dynamic pressure, $\bar{q}\alpha$ during booster burn are shown. This figure shows an additional curve corresponding to the trajectory constrained to $(\bar{q}\alpha)_{max}$ = 67 000 deg-N/m^2 (1400 deg-psf). This case remained on its $(\bar{q}\alpha)_{max}$ boundary for some time, and yet its peak lift of about 900 000 kilograms (2 million pounds) is about the same magnitude as that of the $(\bar{q}\alpha)_{max}$ = 134 000 deg-N/m^2 case. In addition to the very high $\bar{q}\alpha$ peak for the unconstrained case as previously stated, note that the nonlifting case had fairly substantial negative values of $\bar{q}\alpha$ in order to maintain zero lift during booster burn. It should also be observed that for the lifting case $(\bar{q}\alpha)_{max}$ occurs before $\bar{q}_{max}$, while for the nonlifting case $(\bar{q}\alpha)_{max}$ and $\bar{q}_{max}$ occur at the same time.

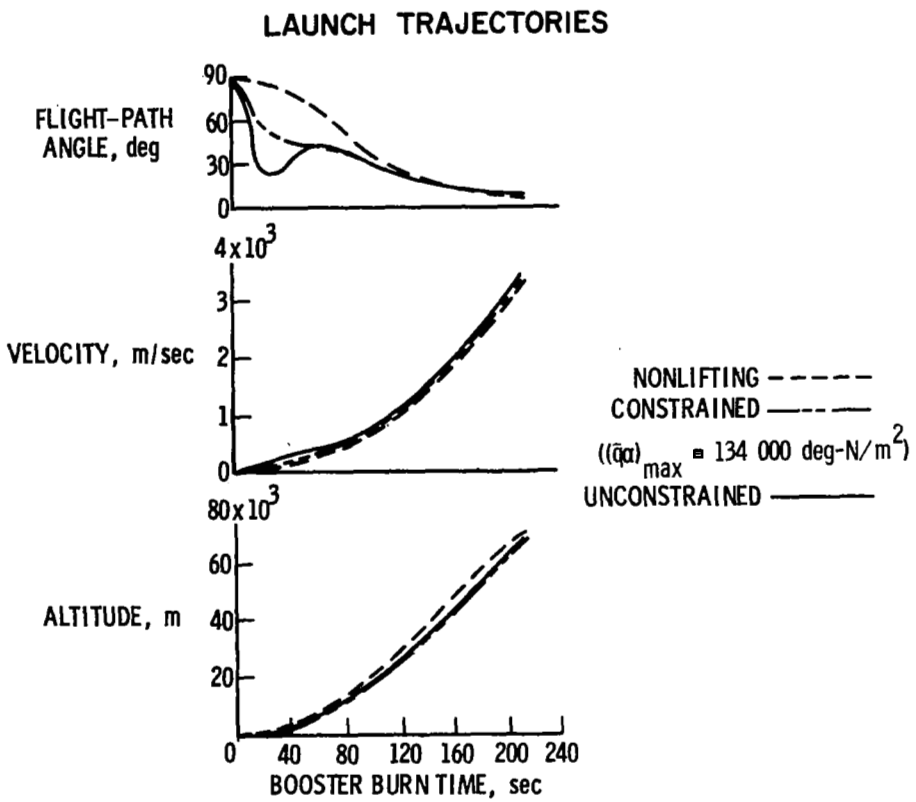

Figure 11

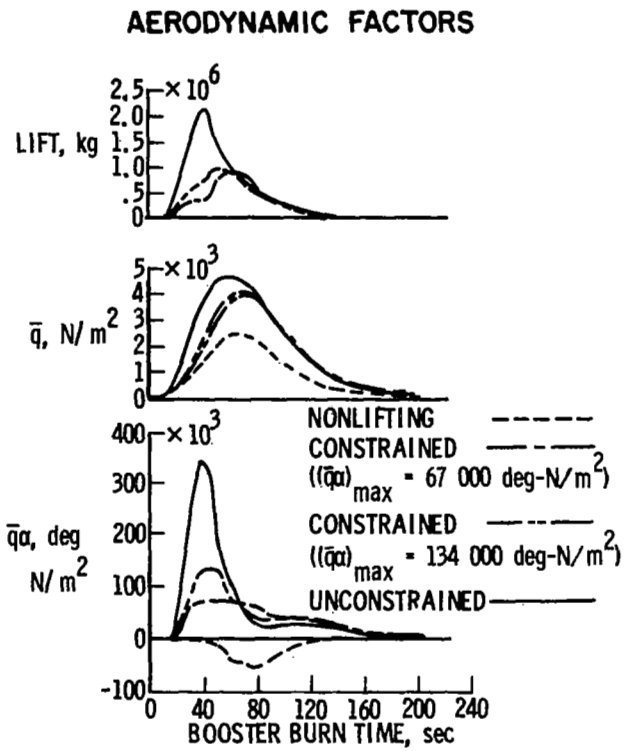

Figure 12

OPTIMAL POINTING-LIFTING

In order to separately evaluate the effects of lifting and thrust pointing, a brief computer study was conducted in which the allowable $\bar{q}\alpha$ was limited to 134 000 deg-N/m^2. For one trajectory, the effects of lift were eliminated by artificially setting the lift and induced drag coefficients to zero. As shown in figure 13, this case then showed a payload improvement of some 1700 kilograms over the nonlifting case, and yet showed some 1800 kilograms less than when the lift and induced drag effects were included in the computations. It is thus surmised that about 50 percent of the improvement was due to the ability to optimally point the thrust vector in relation to the path and that about 50 percent was due to the additional ability to utilize lift.

OPTIMAL POINTING–LIFTING

TRAJECTORY TYPE	PAYLOAD, kg	DELTA PAYLOAD, kg
$\alpha(t)$ FOR ZERO LIFT	18 100	—
OPTIMAL POINTING, NO LIFTING	19 800	1700
OPTIMAL POINTING AND LIFTING	21 600	3500

Figure 13

HEATING RATE

One of the factors which shuttle designers are concerned about, and which has not yet been mentioned, is the heating load experienced by the vehicle. One measure of the heating load is the laminar stagnation-point heat rate for a sphere of unit radius and its integral. The heat rate, in watts/m^2, is shown plotted against time in figure 14 for each of the cases previously mentioned. Tabulated values of the integral of this relation at booster and orbiter burnout times are given in the insert. Note that the heating rates during orbiter burn have been somewhat reduced by the use of lifting trajectories. The heating rates are increased during booster burn but those rates may not be a critical item in the booster. A close examination of the tabulated results shows that the orbiter stage experiences a slightly less severe environment on lifting trajectories than on nonlifting trajectories.

HEATING RATE TIME-HISTORY COMPARISON

TRAJECTORY	LINE TYPE	HEATING INTEGRAL IN JOULES/m^2 AT t =	
		214 sec	426 sec
NONLIFTING	– – – – –	8 115 000	29 275 000
CONSTRAINED	— – – —	12 150 000	31 935 000
UNCONSTRAINED	———	12 285 000	31 710 000

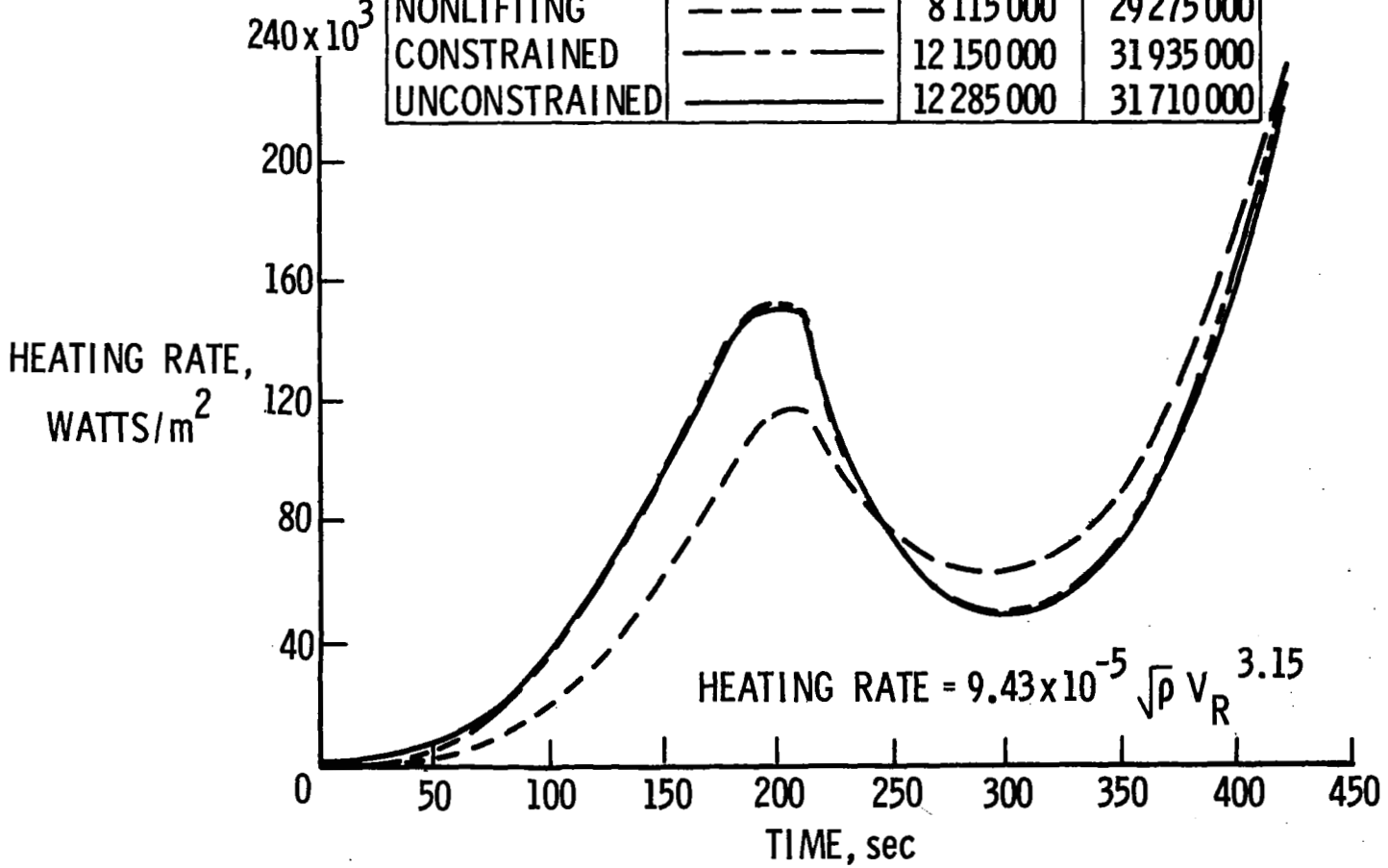

Figure 14

CONCLUDING REMARKS

During ascent the booster-orbiter configuration needs to create about 900 000 kilograms of lift. This should not be a factor of concern since the booster alone is structurally designed for lift loads of about 1.36 million kilograms (3 million pounds). For a configuration of this type, the inertia loads created by the orbiter on the booster during the lifting trajectories would require a more careful examination.

In summary, the use of lifting trajectories, with reasonable values of the airload parameter $(\bar{q}\alpha)_{max}$ can result in payload increases on the order of 15 to 20 percent without undue detrimental effect.

REFERENCES

1. Elliott, Jarrell R.; and Rau, Timothy R. Optimal Payload Trajectory Characteristics for Horizontally Launched Vehicle. J. Spacecraft Rockets, vol. 5, no. 2, Feb. 1968, pp. 218-220.

2. Stein, Laurence H.; Matthews, Malcolm L.; and Frenk, Joel W.: STOP - A Computer Program for Supersonic Transport Trajectory Optimization. NASA CR-793, 1967.

3. Minzner, R. A.; Champion, K. S. W.; and Pond, H. L.: The ARDC Model Atmosphere 1959. AFCRC-TR-59-267, U.S. Air Force, Aug. 1959.